ELSEVIER

Chemical Engineering Science 62 (2007) 2890–2904

Chemical Engineering Science

www.elsevier.com/locate/ces

Techniques for the reconstruction of a distribution from a finite number of its moments

V. John[a], I. Angelov[b], A.A. Öncül[c], D. Thévenin[c,*]

[a]*FR6.1-Mathematik, Universität des Saarlandes, 66041 Saarbrücken, Germany*
[b]*Max-Planck-Institut für Dynamik komplexer technischer Systeme, Arbeitsgruppe System- und Regelungstheorie, 39106 Magdeburg, Germany*
[c]*Laboratory of Fluid Dynamics and Technical Flows, University of Magdeburg "Otto von Guericke", 39106 Magdeburg, Germany*

Received 4 September 2006; received in revised form 26 February 2007; accepted 27 February 2007
Available online 7 March 2007

Abstract

The reconstruction of a distribution knowing only a finite number of its moments is an extremely important but in practice still unsolved question for many fields of science (chemical and process engineering, electronic engineering, nuclear physics, image analysis, biotechnology...). Several methods have been proposed and corresponding mathematical formulations have been introduced in the literature during the last decades. Nevertheless, all these are generally limited to particular, often simple cases and require specific assumptions. It is indeed extremely difficult from a theoretical point of view (it is necessary, however, not sufficient, that all moments are available for a correct reconstruction) as well as from a practical point of view (ill-posed inverse problem) to find an accurate and relatively fast method which can be applied to all scientific areas. In the present paper, different possible methods (prescribed functions, discrete method, spline-based reconstruction) allowing such a reconstruction are explained, compared in terms of efficiency and accuracy, and validated for chemical engineering applications using examples with different degrees of difficulty.

Keywords: Particulate processes; Population balance; Model reduction; Mathematical modeling; Reconstruction of a function

1. Introduction and state of the art

1.1. Possible applications

In the last decade, a renewed interest can be observed in the scientific community dealing with chemical engineering applications concerning moment-based determination of distributions, e.g., particle size distributions (PSD). This is in particular due to the fact that, when external features like turbulent flow properties play an important role for the process under investigation, fast and numerically efficient methods must be employed to describe the population interacting with this flow. Acceptable computational costs are typical for the standard method of moments (MOM) and for related approaches like the quadrature method of moments (QMOM) and its direct alternative (DQMOM) (Marchisio and Fox, 2005). For all such methods, only a finite number of moments associated with the real distribution are finally determined by the numerical procedure. Therefore, after having computed these moments, it is necessary to reconstruct in the best possible way the full, real distribution corresponding to the resulting PSD. Since the PSD generally constitutes the key result to judge the quality of the process, the high importance of the reconstruction procedure appears clearly.

It is also possible to derive the value of different moments indirectly through experimental measurements, since the particle sizing devices provide general knowledge about e.g., the mean particle size or complete PSD. Once the PSD has been measured the corresponding moments (such as zeroth-order moment μ_0, Marchisio et al., 2002) can then be readily computed using the distribution. Moreover, mean particle size data,

* Corresponding author. Tel.: +49 391 6718570; fax: +49 391 6712840.
E-mail addresses: john@math.uni-sb.de (V. John), iangelov@mpi-magdeburg.mpg.de (I. Angelov), Alper.Oencuel@vst.uni-magdeburg.de (A.A. Öncül), Dominique.Thevenin@vst.uni-magdeburg.de (D. Thévenin).

0009-2509/$ - see front matter © 2007 Elsevier Ltd. All rights reserved.
doi:10.1016/j.ces.2007.02.041

which are mostly defined as the ratio of two moments (like $d_{43} = \mu_4/\mu_3$, see Bałdyga and Orciuch, 2001; Marchisio et al., 2001 and $d_{32} = \mu_3/\mu_2$, see Chen et al., 1996) may also represent useful information to determine the moments.

This inverse problem is well-known and has been often considered for more than a century (von Smoluchowski, 1917), not only in the field of chemical engineering. This issue is for example essential for many aspects of image processing (Sluzek, 2005), for determining the magnetic moment from simple experiments (Berkov et al., 2000) or for obtaining the electronic structure of specific materials (Bandyopadhyay et al., 2005). All such contributions are of course very interesting and introduce techniques, like for example the maximum entropy (MaxEnt) method (Bandyopadhyay et al., 2005), which can be also useful for chemical processing applications (Sanyal et al., 2005). Nevertheless, they also often rely on specific approximations or formulations, which might lead to severe restrictions or unnecessary overhead for chemical engineering.

No satisfactory unified method for reconstructing a function using only a finite number of its moments can be found in the literature up to now. For most researchers in chemical engineering dealing with fundamental aspects, this is due to the fact that, mathematically, all the moments up to infinity are requested in order to obtain a perfect reconstruction. Furthermore, the knowledge of all moments is only sufficient if the class of functions in which the reconstruction is sought is restricted appropriately. Considering, e.g., functions which are defined in $[0, \infty)$ and allowing infinitely many oscillations in a neighborhood of 0 or allowing the derivatives of the function to be unbounded in a neighborhood of 0, it can be shown that even the knowledge of all moments is not sufficient to determine a function uniquely (see for example the very interesting publication, McGraw et al., 1998, for concrete examples and further details).

Therefore, the problem of reconstructing a function using a finite number of its moments requires an a priori restriction of the class of functions where the solution is sought. The number of parameters requested to determine the distribution within this class should correspond to the available number of known moments. Following this guideline, chemical engineers dealing with applications generally assume a very simple a priori shape for the distribution (Gaussian, log-normal, β-function, etc.), so that only a very small number of moments are needed to determine the best fit within this assumed class of functions. In this paper, this efficient but limited method will be first discussed before introducing alternative, more general approaches. All presented techniques have been coded as script files using the commercial program MATLAB. These scripts have been used to carry out all the computations presented in the paper.

1.2. Mathematical literature

The problem of reconstructing a function from a given number of moments is known in mathematics as the *finite-moment problem*. It was first studied by Chebyshev (1961) and it can be regarded as a finite dimensional version of the Hausdorff moment problem (Shohat and Tamarkin, 1943). The finite-moment problem is severely ill-conditioned because of the ill-posedness of the Hausdorff moment problem (Frontini et al., 1988; Inglese, 1988; Talenti, 1987). This issue is also related to the inversion of the discrete Laplacian transform (Bertero et al., 1985).

Several approaches for the reconstruction have been proposed in the mathematical literature. In Inglese (1994), piecewise constant functions are studied (splines of order $l = 0$). However, there are severe restrictions on the function to reconstruct: it should be non-negative and moreover non-decreasing. These properties are not given for usual PSDs. For the case considered in Inglese (1994), it was proved that a suitable choice of the nodes of the underlying grid is essential for obtaining a good reconstruction. In addition, numerical tests were reported, which indicate that a similar behavior holds for higher-order splines. But this statement could not be proved. In Inglese (1995), the unknown function is reconstructed with Christoffel functions.

In Tagliani (1999, 2001), the finite-moment problem is studied for the maximum entropy approach, i.e., a real-valued function $f(x) : [0, 1] \to \mathbb{R}_+$ is sought such that the first moments of f coincide with given values and the (Shannon) entropy

$$H[f] := \int_0^1 f(x) \ln[f(x)] \, \mathrm{d}x \tag{1}$$

becomes maximal. This is a constraint optimization problem which can be tackled by the Lagrange multiplier approach. The existence and uniqueness of a solution, the convergence as the number of given moments increases and the stability of the problem with respect to data errors in the given moments are studied or put into a unified framework. It turns out that the problem is ill-posed and therefore the computation of f is ill-conditioned. However, it is shown in Tagliani (2001) that the computation of functionals of f like

$$\int_0^1 F(x) f(x) \, \mathrm{d}x, \tag{2}$$

where $F(x)$ is some known function of physical interest, is well conditioned and can be computed reliably. Nevertheless, extensive numerical tests cannot be found in Tagliani (1999, 2001).

The finite-moment problem has been studied in the mathematical literature almost exclusively from the theoretical point of view. To our best knowledge, the development of general but efficient numerical algorithms has not been completed. For this reason, extensive numerical studies are not available.

1.3. Approaches for moment-based reconstruction

Three different reconstruction methods are presented and investigated in the present paper. The ultimate goal of our work consists in the development of numerical algorithms which are able to obtain a good approximation of any realistic distribution using a finite number of its moments in a stable manner and at acceptable computational costs.

Section 2 presents the test examples used to evaluate the different methods considered in this work.

In Section 3, results obtained with two techniques already available in the literature will be introduced. First, reconstruction using a priori basic shapes for a distribution is presented in order to illustrate the advantages (fast and easy computations) and drawbacks (limitation to simple shapes, a priori knowledge needed about the solution) of this approach. A discrete method based on a time-dependent update of the distribution together with (or possibly after) the computation of the moments is then introduced. This method is very fast, numerically efficient and easy to implement, but cannot be extended to all possible physical processes encountered in chemical engineering. In the presented example, by solving numerically the moment equations, the trajectories of the system are determined and can be used to recover the time-dependent birth and nucleation profiles during the process. Knowing the initial particle distribution, a numerical algorithm is then implemented to add new particles and shift appropriately the existing ones. This is an extension of the method presented in Giaya and Thompson (2004).

In Section 4, a new, highly flexible algorithm based on low-order splines is presented to solve the reconstruction problem. In this approach, no a priori hypotheses concerning the shape and the extent (mathematically, the support) of the distribution are requested. In addition, any number of moments can be used for the reconstruction. The advantages, drawbacks, practical implementation and possible improvements of this approach will be discussed in detail.

Further interesting issues concerning reconstruction and possibilities to solve the inverse finite-moment problem can be found in the literature but are not further investigated in the present work. Interested readers should refer to the publications cited below for details. The already mentioned maximum entropy method (see for example Bandyopadhyay et al., 2005; Myers and Hanson, 1990; Gzyl, 2000) is a powerful and quite flexible technique, but has not been tested in detail for chemical engineering problems to our knowledge. In Diemer and Olson (2002) and Diemer and Ehrman (2005), a non-linear regression method based on the minimization of the root-mean-square-error of the expansion of the solution in a set of orthogonal basis functions is employed for the reconstruction. The main difficulty here is the identification of a suitable set of orthogonal functions. In Diemer and Ehrman (2005), modified γ-functions are employed for this purpose. First numerical tests show that at least 10 moments of the distribution are needed to get acceptable reconstructions.

2. Examples considered as test-cases for the reconstruction

The ith moment of a function $f(t,x) : [0,\infty) \to \mathbb{R}$ is classically defined by

$$\mu_i(t) = \int_0^\infty x^i f(t,x)\,\mathrm{d}x, \quad i = 0, 1, 2, \ldots . \tag{3}$$

Since practical distributions contain only non-negative values, the further analysis is restricted to such types of functions. If $f(t,x)$ represents for example the PSD for a crystallization process, the zeroth moment μ_0 corresponds to the overall number of crystals, while the third moment μ_3 is proportional to the volume of the crystalline material in the crystallizer.

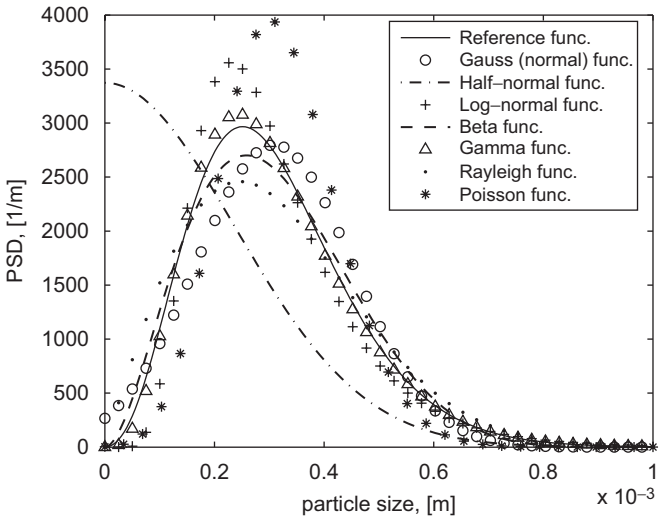

Fig. 1. Reconstructed distributions obtained with various a priori shape functions for Example 2.1. The solid line corresponds to the exact solution, used to compute numerically the moments.

Four test-cases of increasing complexity will be considered in what follows. Up to 11 moments will be used for the reconstruction. All moment values listed below are given in S.I. Units and have been obtained numerically. Experimentally measured moments are not considered in this first study and could lead to new difficulties, since they will be less accurate and will thus contain a much higher level of noise.

Example 2.1 (*Distribution with a single peak*). The first distribution to reconstruct has been produced arbitrarily. As a consequence, the first moment has been simply normalized. The distribution is smooth and shows only a single peak (Fig. 1). The first 11 moments of the corresponding PSD are given by

$$\begin{aligned}
\mu_0 &= 1.0000000000000000e+00,\\
\mu_1 &= 3.0917926803257545e-04,\\
\mu_2 &= 1.1593213204304320e-07,\\
\mu_3 &= 5.0623202094394748e-11,\\
\mu_4 &= 2.5051920275299736e-14,\\
\mu_5 &= 1.3765687884540478e-17,\\
\mu_6 &= 8.2607947507541690e-21,\\
\mu_7 &= 5.3386730929083559e-24,\\
\mu_8 &= 3.6713093994877131e-27,\\
\mu_9 &= 2.6590398851651892e-30,\\
\mu_{10} &= 2.0107822133383323e-33.
\end{aligned} \tag{4}$$

Example 2.2 (*Distribution with two peaks*). The particle mass distribution (PMD) in this example shows two peaks (Fig. 2). It is still smooth but it becomes almost zero between the peaks, so that the peaks are separated. In addition, the left peak is close to the zero-boundary, is considerably higher than the right one and is quite narrow. This distribution is the result of a direct solution obtained by solving a particle balance equation (PBE).

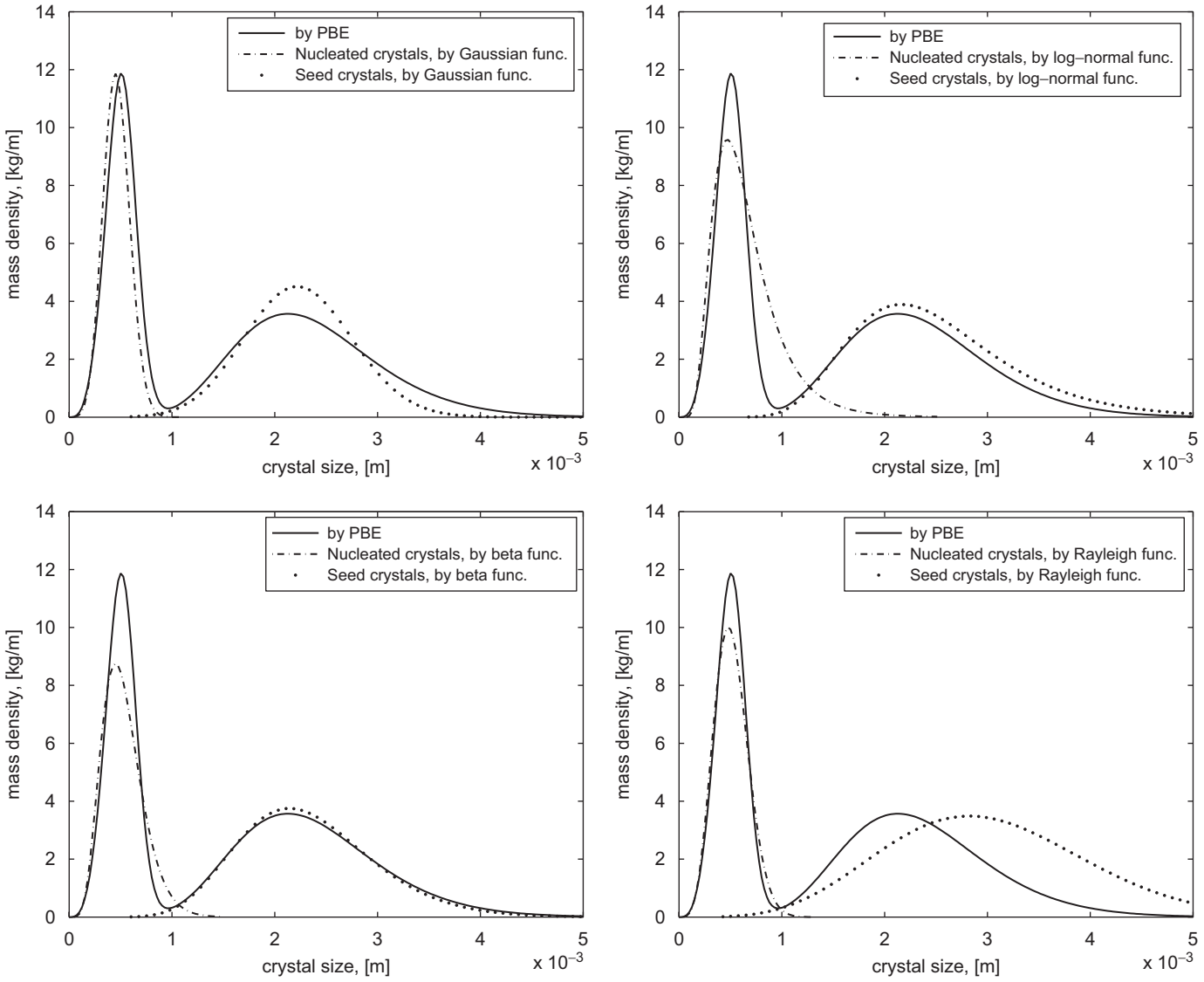

Fig. 2. Example 2.2, direct solution of the PBE, used as a reference (solid line) and moment-based reconstruction based on known functions. Top-left: reconstruction based solely on Gaussian functions. Top-right: reconstruction based solely on log-normal functions. Bottom-left: reconstruction based solely on β-functions. Bottom-right: reconstruction based solely on Rayleigh functions.

Further details can be found in Öncül et al. (2005a,b). Its first moments are

$$\begin{aligned}
\mu_0 &= 1.028571810801850e-02,\\
\mu_1 &= 1.627619528771249e-05,\\
\mu_2 &= 3.731662761082810e-08,\\
\mu_3 &= 1.005399673163290e-10,\\
\mu_4 &= 2.961317428763996e-13,\\
\mu_5 &= 9.324232740417577e-16,\\
\mu_6 &= 3.106813835529885e-18,\\
\mu_7 &= 1.087507001932166e-20,\\
\mu_8 &= 3.973765578013985e-23,\\
\mu_9 &= 1.507036647558311e-25,\\
\mu_{10} &= 5.901352427828747e-28. \qquad (5)
\end{aligned}$$

Example 2.3 (*Distribution with three peaks*). In order to further increase complexity, this example considers a distribution with three peaks (see the right picture in Fig. 5). This example has been created specifically for the present work. It would correspond in practice to a batch seeded crystallization process, when two seed distributions with a different mean size are initially mixed (left picture in Fig. 5). The first moments of this distribution are as follows:

$$\begin{aligned}
\mu_0 &= 5.5911475010957845e+04,\\
\mu_1 &= 9.7447189797086963e+01,\\
\mu_2 &= 2.2713126695535327e-01,\\
\mu_3 &= 6.0281801524505118e-04,\\
\mu_4 &= 1.7044920031329059e-06,\\
\mu_5 &= 5.0010225203552623e-09,
\end{aligned}$$

$$\mu_6 = 1.5051001861147765e-11,$$
$$\mu_7 = 4.6186266332179558e-14,$$
$$\mu_8 = 1.4397849400167651e-16,$$
$$\mu_9 = 4.5478110783254306e-19,$$
$$\mu_{10} = 1.4527644074215552e-21. \quad (6)$$

Example 2.4 (*Distribution with two different-sized, non-smooth peaks*). The distribution considered in this last example is obtained when simulating a preferential crystallization process (Elsner et al., 2005). It shows only two peaks, but they are associated with very different maximum values (the right peak is almost negligible compared to the left one) and the left peak is extremely steep (right picture in Fig. 6). The first moments of the distribution are:

$$\mu_0 = 1.1951949826317582e-02,$$
$$\mu_1 = 1.8240118994119752e-05,$$
$$\mu_2 = 4.1749183311343385e-08,$$
$$\mu_3 = 1.1378087759074244e-10,$$
$$\mu_4 = 3.4031387152032602e-13,$$
$$\mu_5 = 1.0920182412236499e-15,$$
$$\mu_6 = 3.7265448687225173e-18,$$
$$\mu_7 = 1.3442843240712988e-20,$$
$$\mu_8 = 5.0978673694936700e-23,$$
$$\mu_9 = 2.0215211667243400e-25,$$
$$\mu_{10} = 8.3393525030070373e-28. \quad (7)$$

3. Reconstructing a distribution using known techniques

3.1. Reconstruction by parameter fitting when assuming a priori a simple shape

In this section, reconstructing a distribution using a priori elementary shapes is considered in order to illustrate the advantages (fast and easy computations) and drawbacks (limitation to simple shapes, a priori knowledge needed about the solution) of this technique.

Indeed, the fastest and the easiest method to reconstruct a distribution knowing only some of its moments is fitting it to a prescribed mathematical function (such as Gaussian, log-normal, β-function, etc., Heinz, 2003; Mersmann, 2001) by using a small number of low-order moments, obtained for example numerically with the standard method of moments (MOM), first proposed by Hulburt and Katz (1964) and used since then by many authors (Bałdyga and Orciuch (2001), Ramkrishna (2000), Fox (1998) and Öncül et al. (2006)). The MOM has been also employed in Giaya and Thompson, 2004 and further extended to more general versions (QMOM in McGraw, 1997 and DQMOM in Marchisio and Fox, 2005), since the MOM has been shown to be inappropriate or insufficiently accurate for a number of cases. Even if these newer methods are more general in nature, the reconstruction of the PSD must be carried out exactly in the same manner as using MOM. A reconstruction based on known functions is in that case a quite powerful and fast method, allowing quite often the determination of single-peak PSDs with an excellent accuracy. A PSD with several, clearly separated peaks can be reconstructed using a superposition of single-peak reconstructed PSDs, as demonstrated below.

Usual a priori functions employed for PSD reconstructions in the literature are in particular Gaussian (or normal), half-normal, log-normal, β (beta), γ (gamma), exponential, Rayleigh and Poisson functions. Among those, the Gaussian function is probably the most common one, also widely applied in natural and social sciences. One characteristic property of this function is its symmetrical distribution about the mean. However, this property directly leads to the presence of particles with negative sizes. The corresponding amount is sometimes negligible and can be truncated, but this is not necessarily always the case and can lead to non-physical properties (Bałdyga and Bourne, 1999). The half-normal function is a special form of the Gaussian function with a mean of zero and a distribution containing only the positive (physical) particle sizes (i.e., neglecting the negative half of the curve). This function could for instance represent the number distribution of particles in an incomplete crystallization process, where the bulk of the particles are the newly nucleated ones, which are highly accumulated near the zero size, considered as the theoretical size of a newly nucleated, molecule-like particle.

In some cases, a symmetric distribution for a reconstruction is not desirable at all. One of the classical functions for such cases is the log-normal function, which can display a long tail in the direction of the larger particle sizes. Due to its shape, this function is widely used in powder, spray and aerosol technologies. Another function often used in particle technology is the γ-function that can take various shapes depending on the skewness and kurtosis values deduced from the corresponding moment data (Heinz, 2003). The exponential function is a special case of the γ-function, with a mean value equal to the standard deviation. As an alternative, the β-function is capable of taking more various shapes than the γ-function and can thus be used in a slightly more flexible manner. Moreover, this β-function can easily display skew on either side of the distribution peak, unlike the log-normal and γ-functions. Therefore, this function is widely used in engineering applications, for example to model turbulent flows, or in particle and combustion technologies. The Rayleigh function is mostly used in radioactivity and wind energy technology. Finally, the Poisson function is a discrete distribution and can in principle only be considered when the particle sizes are chosen from discretized values.

All mentioned functions are listed below for the sake of completeness. For this purpose, a few general distribution properties like mean size ($\overline{x}$), coefficient of variation (c_v) and standard deviation (σ) must first be defined in terms of the first three moments (μ_j, $j = 0, 1, 2$):

$$\overline{x} = \frac{\mu_1}{\mu_0}, \quad (8)$$

$$c_v = \sqrt{\frac{\mu_0 \mu_2}{\mu_1^2} - 1}, \quad (9)$$

$$\sigma = \overline{x} c_v. \quad (10)$$

The various distributions mentioned above are then characterized as follows, with all moments necessary for their computation listed in an explicit manner:

1. Gaussian (normal) function (three moments needed; μ_0, μ_1, μ_2):

$$f(x) = \frac{1}{\sigma\sqrt{2\pi}} \exp\left(-\frac{(x-\overline{x})^2}{2\sigma^2}\right). \tag{11}$$

2. Half-normal function (three moments needed; μ_0, μ_1, μ_2):

$$f(x) = \frac{2\phi \exp(-x^2\phi^2/\pi)}{\pi} \quad \text{where } \phi = \sqrt{\frac{\pi-2}{2\sigma^2}}. \tag{12}$$

3. Log-normal function (three moments needed; μ_0, μ_1, μ_2):

$$f(x) = \frac{1}{x \ln \sigma_g \sqrt{2\pi}} \exp\left(-\frac{\ln^2(x/\overline{x}_g)}{2\ln^2 \sigma_g}\right)$$
$$\text{where } \overline{x}_g = \frac{\overline{x}}{\exp(0.5\ln^2 \sigma_g)},$$
$$\sigma_g = \exp(\sqrt{\ln(c_v^2+1)}). \tag{13}$$

4. γ-function (three moments needed; μ_0, μ_1, μ_2):

$$f(x) = \frac{\mu^\mu x^{(\mu-1)} \exp(-\mu x/\overline{x})}{\Gamma(\mu)\overline{x}^\mu}$$
$$\text{where } \mu = \frac{\overline{x}^2}{\sigma^2} \quad \text{and} \quad \Gamma(\mu) = \int_0^\infty z^{\mu-1} e^{-z}\, dz. \tag{14}$$

5. β-function (three moments needed; μ_0, μ_1, μ_2):

$$f(x) = \frac{x^{(\alpha-1)}(1-x)^{(\beta-1)}}{B(\alpha,\beta)}$$
$$\text{where } \alpha = \overline{x}\left(\frac{\overline{x}(1-\overline{x})}{\sigma^2} - 1\right),$$
$$\beta = (1-\overline{x})\left(\frac{\overline{x}(1-\overline{x})}{\sigma^2} - 1\right)$$
$$\text{and } B(\alpha,\beta) = \frac{\Gamma(\alpha)\Gamma(\beta)}{\Gamma(\alpha+\beta)}. \tag{15}$$

6. Exponential function (two moments needed; μ_0, μ_1):

$$f(x) = \frac{\exp(-x/\overline{x})}{\overline{x}}. \tag{16}$$

7. Rayleigh function (two moments needed; μ_0, μ_1):

$$f(x) = \frac{x\exp(-0.5x^2/s^2)}{s^2} \quad \text{where } s = \overline{x}\sqrt{\frac{2}{\pi}}. \tag{17}$$

8. Poisson function (two moments needed; μ_0, μ_1):

$$f(x) = \frac{\overline{x}^x e^{-\overline{x}}}{x!}. \tag{18}$$

In order to illustrate the advantages and drawbacks of this approach, it is sufficient to consider two of the four examples presented in Section 2.

Example 2.1: For this first, simple example, all functions mentioned above (except for the exponential function, which is only a special case of a γ-function) have been used to reconstruct the distribution (see Section 2 for the corresponding set of moments). In this way it is possible to get a feeling for the typical form associated with each of these functions. The results are presented in Fig. 1. As one can see, the reference PSD is best represented by the γ-function in this particular case, with a maximum relative error well below 10%. It is interesting to note that the Gaussian function leads here to a non-negligible amount of particles with a negative size. Moreover, the half-normal distribution leads to the largest error for this particular case.

Example 2.2: Due to the fact that the resulting distribution is an essential criterion for assessing the properties and quality of a product (Mersmann, 2001), the assumed shape of the curve must of course accurately fit the corresponding data. The resulting accuracy can be measured quantitatively by comparing either to a direct, reference solution of the corresponding PBEs or to experimental results. To illustrate this procedure, such a comparison is presented in Fig. 2 for the two-peaked PMD of Example 2.2, comparing the direct solution of the PBE (reference solution, see Öncül et al., 2005a,b) with the reconstruction based on some known functions selected from the above list: Gaussian, log-normal, β- and Rayleigh functions. Here, the two peaks correspond, respectively, to nucleated crystals (left part, smaller size, higher peak) and to initial seed crystals after growth during a crystallization process (right part, larger size, lower peak). In that case, the reference solution of the PBE delivers directly the two peaks, while the reconstruction procedure is carried out separately for each peak, based on two separate sets of moments. These two sets are obtained numerically from the reference solution of the PBE and are given by

Left peak	Right peak
$\mu_0 = 4.317540326711211e-3$	$\mu_0 = 5.968174268753386e-3$
$\mu_1 = 2.179025715100396e-6$	$\mu_1 = 1.409715130777033e-5$
$\mu_2 = 1.190570221859969e-9$	$\mu_2 = 3.612596957795690e-8$

The interest of separating in this manner the different parts of a distribution has already been pointed out in the past, for example in McGraw et al. (1998). As can be seen in Figs. 2 and 3, the Gaussian function reproduces the shape of the nucleated crystals most exactly among the selected functions, showing that the nucleated crystals have a rather symmetric distribution. On the other hand, the crystals initially introduced as seeds at the beginning of the process are best represented by the β-function. This is not a surprise since the experimentally measured distribution of the initial seed crystals is already very close to a β-function shape (Öncül et al., 2005a; Elsner et al., 2005). In this case the γ-function (not shown for clarity) is almost identical with the β-function. The previously explained characteristic property of the log-normal function (i.e., the long tail in the direction of the larger sizes) can be clearly seen in Fig. 2, especially for the nucleated crystals. This property causes a large overlap between the distribution of the nucleated crystals and the seed crystal distribution, leading to a considerable error when adding both values to get the global distribution. Finally,

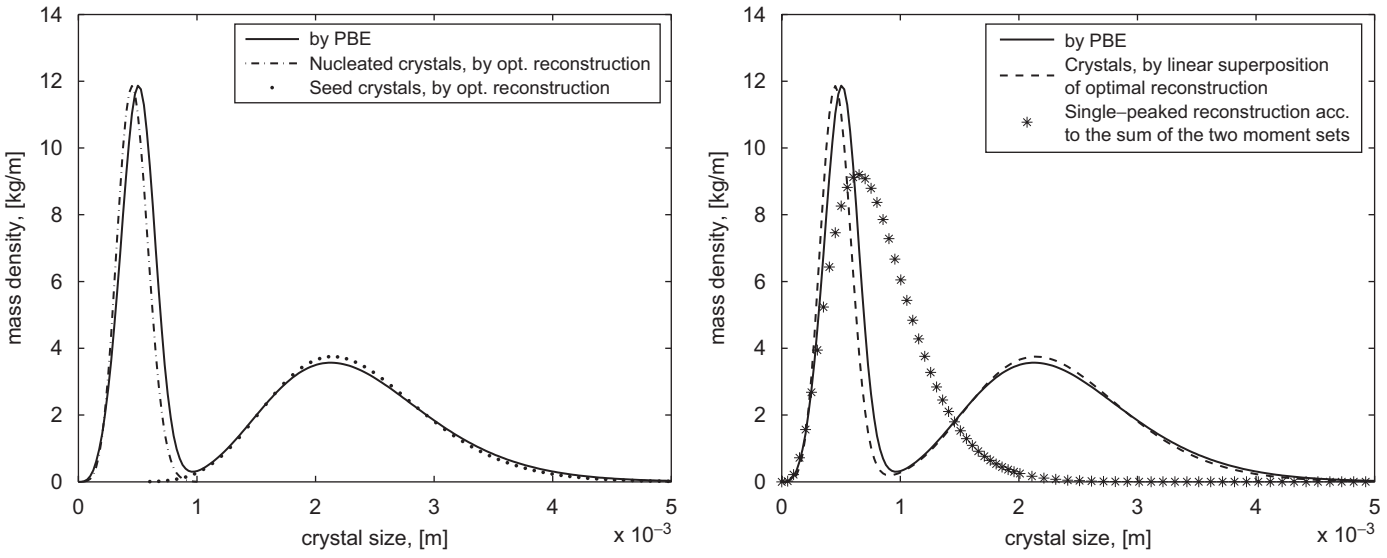

Fig. 3. Example 2.2, best possible combination for reconstruction based on a priori function shape (Gaussian function for nucleated crystals and β-function for seeds after growth). Left: separately fitted single-peaked curves. Right: linear superposition of both distributions (dashed line) and the resulting single-peaked distribution (based on β-function, star symbols) when the single set of moments equal to the sum of the two separate moment sets would have been used.

the Rayleigh function underestimates the peak values of the nucleated crystals and shows a considerable offset toward the larger particle sizes for the seed crystal distribution. The reconstructed, global PMD obtained by superposition is in general not smooth at the intersection of the two separate curves.

For all these reconstructions, the sets of only the first three moments of both nucleated and seed crystals are separately needed for the fitting procedure, so that the corresponding population models are easily solved for. However, separate sets of moments are often not available in practice. Moreover, the approach of using separate sets of moments works only if the peaks are well separated. If only one set of moments equal to the sum of the two separate moment sets would have been used, the resulting reconstruction would then give a single-peaked curve and thus a poor description of the PMD, as shown in the right picture in Fig. 3. It is also worth reminding that all these reconstructed curves correspond of course to exactly the same first three moment sets but show obviously very different shapes. This underlines the importance (and the difficulty) of the reconstruction process. Even if the corresponding population balance model would deliver accurate final data with respect to the particle properties expressed in terms of moments, the reconstructed distribution might not be accurate at all, if not enough moments are available or if a bad reconstruction procedure is used. As explained previously, the issue of completely different distributions corresponding to the same moments is considered in more details in McGraw et al. (1998). Choosing the appropriate function is a major issue and can only been done by considering reference data.

Fig. 3 illustrates the best possible combination of the reconstructed PMDs for this particular example. The left picture shows the fitted curves separately, whereas the right one depicts the linear superposition of these two distributions (dashed line), demonstrating an excellent agreement. Results for Examples 2.3 and 2.4 are not presented since they do not lead to any supplementary information. The interested reader can find other comparisons in John et al. (2005).

The reconstruction of a distribution using a few low-order moments and considering an a priori assumed function shape is a very efficient method, since the solution is obtained immediately and without any time-consuming computation. The obtained accuracy can be very high (relative error of a few %) when using the correct functional shape. But this method requires a lot of information concerning the expected distribution. Thus, this method is only accurate and should always be retained when the properties of the final PSD or PMD are quite well known (for example when considering a small variation compared to a known process). On the other hand, when considering an application with unknown distribution, this method cannot reasonably be retained in general. In that case, alternatives must be considered.

3.2. Discrete method

A discrete method based on a time-dependent update of the distribution together with or after the computation of the moments is now presented. A similar approach has been first reported in Giaya and Thompson (2004), where it has been used for an unseeded batch cooling crystallizer.

A simplified dynamic model of an ideally mixed seeded batch crystallizer is obtained by assuming an overall size-independent growth rate $G(t)$ and an overall nucleation rate $B(t)$. Phenomena like attrition, breakage and agglomeration are neglected. Under these assumptions, the resulting population balance is (Ramkrishna, 2000):

$$\frac{\partial F(t,x)}{\partial t} = -G(t)\frac{\partial F(t,x)}{\partial x}, \tag{19}$$

where t is time, x represents the characteristic particle size and $F(t, x)$ is the number density function. The following boundary and initial conditions apply:

$$F(t, 0) = \frac{B(t)}{G(t)}, \quad F(0, x) = F_{\text{seeds}}(x), \tag{20}$$

where $F_{\text{seeds}}(x)$ is the form of the initial seeds distribution.

The mass balance of the liquid phase is modeled by an integro-differential equation:

$$\frac{\mathrm{d}m_{\text{liq}}(t)}{\mathrm{d}t} = -3\rho_s k_v G(t) \int_0^\infty x^2 F(t, x)\,\mathrm{d}x. \tag{21}$$

The growth rate $G(t)$ is assumed to depend on the supersaturation only and is described by a simple power-law equation:

$$G(t) = k_g (S - 1)^g. \tag{22}$$

Here, k_g is an overall crystal growth rate constant and S denotes the actual degree of supersaturation.

If crystals are already dispersed in the crystallizing medium, secondary nucleation can occur at supersaturation levels which are significantly lower than those at which primary nucleation takes place (Mersmann, 2001). Its rate can then be described by an overall power-law expression

$$B(t) = k_b (S - 1)^b \int_0^\infty x^3 F(t, x)\,\mathrm{d}x, \tag{23}$$

where k_b is generally assumed to be related to the stirring power.

The distributed model (19)–(23) can be considerably simplified by converting it into a moment-based model (Randolph and Larson, 1988). From the PDE (19) with the boundary condition (20), a set of ODEs for the moments of the PSD can be derived. By partial integration, it follows from (19), (20) that

$$\frac{\mathrm{d}\mu_0(t)}{\mathrm{d}t} = B(t), \quad \frac{\mathrm{d}\mu_i(t)}{\mathrm{d}t} = i G(t) \mu_{i-1}(t), \quad i = 1, 2, \ldots . \tag{24}$$

In the present approach, only the first four moments are used, as they can be calculated independently from the higher moments. The solution of this system is not expensive in terms of computational time, but it describes accurately only the dynamics of the overall characteristics of the PSD. The information on the internal property (in this case the distribution of the crystal size x) is lost after applying the transformation involving only the moments. However, the form of the PSD can be recovered by a simple numerical algorithm, which exploits the following assumptions: (1) nucleation at negligible particle size, as used in (20), (2) no breakage or agglomeration, (3) the PSD evolves only by growth, see (22).

The numerical solution of the reduced system (21)–(24) delivers information about the mass of the dissolved material $m_{\text{liq}}(t)$ at discrete time instances Δt during the batch process. Using Eqs. (22) and (23), the corresponding growth and nucleation rate for each time instance can be calculated. Using the recovered growth and nucleation time trajectories, the profile of the boundary condition (20) can be recovered, too. This is sufficient to reconstruct the final PSD.

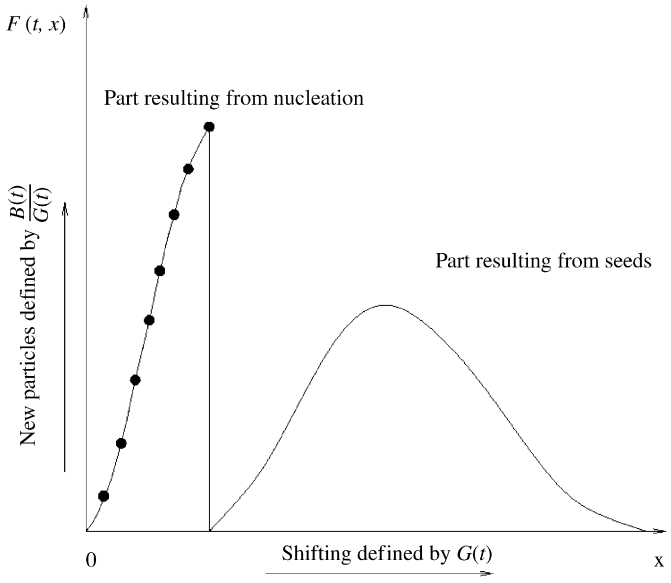

Fig. 4. Particle size recovery by discrete method.

The recovery procedure starts from the size-discretized initial condition $F_{\text{seeds}}(x)$. For each time step Δt, particles at zero size are added, according to the boundary condition profile, and shifted towards larger sizes, according to the growth rate profile. Fig. 4 illustrates this process. Reconstruction examples are now described.

Example 2.3: On the left part of Fig. 5, the employed, known distribution of the initial seeds is presented. The dotted line on the right picture presents the numerical solution of the PBE, where the spatial variable is discretized using backward differences. This scheme of discretization is stable, but also introduces a significant amount of numerical diffusion. The dashed line on the same figure presents the numerical solution of the distributed model using the high-resolution semi-discrete scheme of Koren (Qamar et al., 2006) on a uniform grid. The resulting final distribution is well resolved, the sharp edge (resulting from burst of nucleus when the seeds are added in the supersaturated solution) is preserved. The solid line on the right picture presents the recovered PSD by the discrete method. Only the temporal evolution of the first four moments has been used. The resulting final distribution shows a good agreement with the solution of the high-resolution scheme, but is associated with a considerably smaller computation time.

Example 2.4: The applicability of the proposed algorithm is now tested on a realistic example concerning preferential crystallization (Elsner et al., 2005). Again, the model is based on a number of simplifying assumptions: overall size-independent growth rate $G(t)$, no attrition, no breakage or agglomeration. This allows the use of the simplified dynamic model for the first four moments and the dissolved mass (21)–(24), describing accurately only the overall properties. The high nucleation rate results in a large number of nucleated particles, which is a challenge for the reconstruction of the distribution.

The distribution of the used seeds is presented on the left-hand side of Fig. 6. On the right-hand side of the same figure,

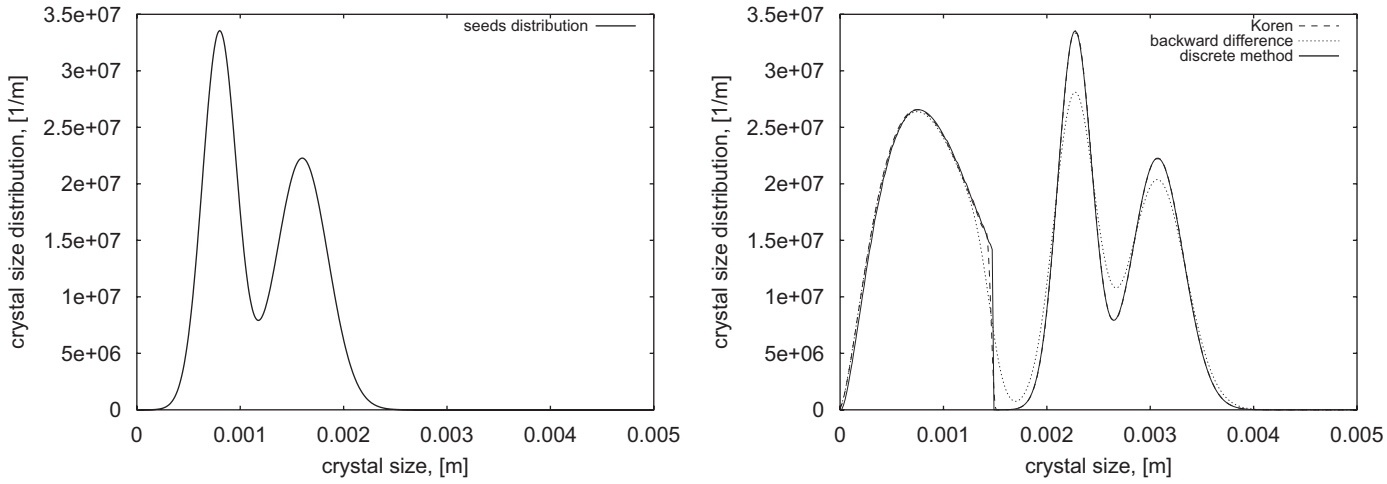

Fig. 5. Example 2.3, solid line, left figure: form of the initial seeds distribution, determined experimentally. Solid line, right figure: discrete method reconstruction using four moments. Dotted line, right figure: numerical solution of the PBE using a backward-difference discretization. Dashed line, right figure: numerical solution of the PBE using Koren's discretization.

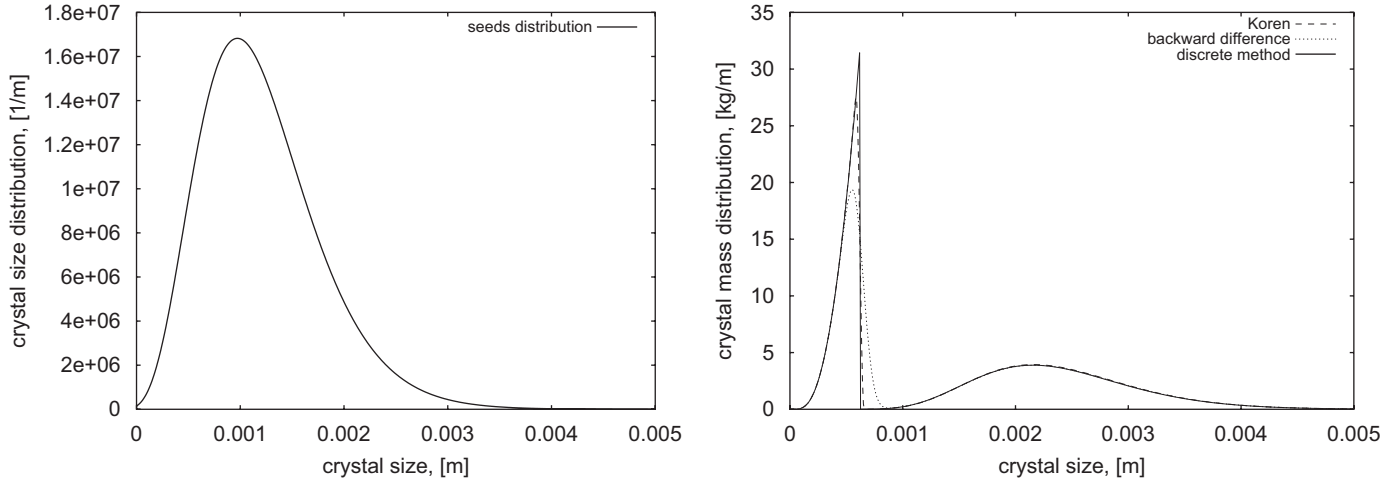

Fig. 6. Example 2.4, solid line, left figure: form of the initial seeds distribution, determined experimentally. Solid line, right figure: discrete method reconstruction using four moments. Dotted line, right figure: numerical solution of the population model using a backward-difference discretization. Dashed line, right figure: numerical solution of the population model using Koren's discretization.

the computed PMD is presented. Again, there is a very good agreement between the distributions obtained from reconstruction using the discrete method (solid line) and the solution of the PBE with the high-resolution scheme of Koren (dashed line), while the backward-difference solution (dotted line) gives smeared results near the discontinuity.

These results demonstrate the good agreement of the discrete reconstruction method with the numerical solution of the distributed PBE model. The discrete method furthermore preserves the initial form of the seeds crystals, which means that this algorithm does not introduce significant numerical diffusion. Its low computational cost makes this algorithm suitable also for online applications like e.g., model-predictive control or state observers when reduced models are used. Further investigations are now being carried out to investigate the possible extension of this approach to problems including other physical phenomena (breakage, agglomeration...).

In spite of the successful comparisons presented in this section, it must be kept in mind that both reconstruction methods introduced up to now request a number of simplifications and hypotheses in order to be applicable. Complementary approaches are therefore clearly needed, as introduced in the next section.

4. The reconstruction of a distribution by splines

Now, splines are considered for the reconstruction of a function whose first L moments are given. Let $x_1 < x_2 < x_3 < \cdots < x_{n+1}$ be discrete points of the x-axis. A spline (piecewise

polynomial) $s^{(l)}(x)$ of degree l has the following properties:

- $s^{(l)}(x)$ is in each subinterval $[x_i, x_{i+1}]$, $i = 1, \ldots, n$, a polynomial of degree l,
- $s^{(l)}(x)$ is $(l-1)$-times continuously differentiable in $[x_1, x_{n+1}]$.

The key features of using a reconstruction by splines are as follows:

- No a priori assumptions on the shape of the function $f(x)$ to be reconstructed are needed. The shape of the function will be approximated by a piecewise polynomial function. The coefficients of the polynomials are computed by solving an ill-conditioned linear system of equations.
- Only a rough a priori information about the interval where $f(x)$ has positive values is needed. An appropriate interval for computing the reconstruction is later on computed iteratively in an automatic manner.
- An arbitrary number of available moments can be used. However, since the reconstruction of a function by a finite number of its moments is a severely ill-conditioned problem, only reliable moments should be used. This is due to the fact (ill-condition) that small changes of the data might (but must not necessarily) lead to rather large changes in the reconstruction. This might be a problem for experimentally measured moments, necessarily associated with a larger uncertainty.

Spline-based reconstruction is considered for $l \in \{1, 2, 3\}$, i.e., linear, quadratic and cubic splines.

4.1. System of equations

The generation of the linear system of equations will be exemplified for cubic splines, i.e., $l = 3$. Let $[a, b]$ be a given interval and $a = x_1 < x_2 < x_3 < \cdots < x_{n+1} = b$. The ansatz is

$$s_i(x) = \sum_{j=0}^{3} s_{ij}(x - x_i)^j, \quad x \in [x_i, x_{i+1}], \quad i = 1, \ldots, n. \tag{25}$$

There are $4n$ unknown coefficients s_{ij} to determine. Because of the regularity assumptions on a cubic spline, it is possible to define

$$s_i'(x) = \sum_{j=1}^{3} s_{ij}\, j (x - x_i)^{j-1},$$
$$s_i''(x) = \sum_{j=2}^{3} s_{ij}(j-1)\, j (x - x_i)^{j-2}. \tag{26}$$

The function $f(x)$ which should be reconstructed is a probability density function. It is assumed that $f(x)$ vanishes identically outside $[x_1, x_{n+1}]$. For the moment, a smooth transition at the boundaries of the interval is assumed (concerning the treatment of non-smooth boundary transitions, see Remark 4.1). This means for the left boundary

$$s_1(x_1) = 0, \quad s_1'(x_1) = 0, \quad s_1''(x_1) = 0. \tag{27}$$

Inserting these conditions into the ansatz (25) gives the following three equations:

$$s_1(x_1) = s_{10} = 0, \quad s_1'(x_1) = s_{11} = 0, \quad s_1''(x_1) = 2s_{12} = 0. \tag{28}$$

Analogously, the right boundary corresponds to

$$s_n(x_{n+1}) = 0, \quad s_n'(x_{n+1}) = 0, \quad s_n''(x_{n+1}) = 0, \tag{29}$$

which gives the following three equations:

$$\begin{pmatrix} 1 & x_{n+1} - x_n & (x_{n+1} - x_n)^2 & (x_{n+1} - x_n)^3 \\ 0 & 1 & 2(x_{n+1} - x_n) & 3(x_{n+1} - x_n)^2 \\ 0 & 0 & 2 & 6(x_{n+1} - x_n) \end{pmatrix} \begin{pmatrix} s_{n0} \\ s_{n1} \\ s_{n2} \\ s_{n3} \end{pmatrix} = \begin{pmatrix} 0 \\ 0 \\ 0 \end{pmatrix}. \tag{30}$$

Now, let us consider the required continuity of $s^{(3)}(x)$ at $x_{i+1} (i = 1, \ldots, n-1)$: $s_i(x_{i+1}) = s_{i+1}(x_{i+1})$. This gives $n-1$ equations of the form

$$(1 \;\; x_{i+1} - x_i \;\; (x_{i+1} - x_i)^2 \;\; (x_{i+1} - x_i)^3 \;\; -1) \begin{pmatrix} s_{i0} \\ s_{i1} \\ s_{i2} \\ s_{i3} \\ s_{(i+1)0} \end{pmatrix} = 0. \tag{31}$$

The next requirement consists in the continuity of the first derivative of $s^{(3)}(x)$ at $x_{i+1} (i = 1, \ldots, n-1)$: $s_i'(x_{i+1}) = s_{i+1}'(x_{i+1})$. This gives another $n-1$ conditions which are of the component-wise form

$$(1 \;\; 2(x_{i+1} - x_i) \;\; 3(x_{i+1} - x_i)^2 \;\; -1) \begin{pmatrix} s_{i1} \\ s_{i2} \\ s_{i3} \\ s_{(i+1)1} \end{pmatrix} = 0. \tag{32}$$

Last, the second derivative of $s^{(3)}(x)$ should be also continuous at $x_{i+1} (i = 1, \ldots, n-1)$: $s_i''(x_{i+1}) = s_{i+1}''(x_{i+1})$. These $n-1$ conditions have the form

$$(2(x_{i+1} - x_i) \;\; 6(x_{i+1} - x_i) \;\; -1) \begin{pmatrix} s_{i2} \\ s_{i3} \\ s_{(i+1)2} \end{pmatrix} = 0. \tag{33}$$

Altogether, the requirements on the cubic spline in Eqs. (28)–(33) give $3(n-1) + 3 + 3 = 3n + 3$ conditions for $4n$ unknowns. That means, $L = 4n - 3n - 3 = n - 3$ additional conditions are still required, which have to come from the known moments.

Considering the kth moment of the spline $s^{(3)}$, $k \in \mathbb{N}$,

$$\begin{aligned}\int_{x_1}^{x_{n+1}} & x^k s^{(3)}(x)\,\mathrm{d}x \\ &= \sum_{i=1}^{n} \int_{x_i}^{x_{i+1}} x^k s_i(x)\,\mathrm{d}x \\ &= \sum_{i=1}^{n} \sum_{j=0}^{3} s_{ij} \int_{x_i}^{x_{i+1}} x^k (x-x_i)^j\,\mathrm{d}x. \end{aligned} \tag{34}$$

Denoting

$$\begin{aligned} I_1 &= \frac{x_{i+1}^{k+1} - x_i^{k+1}}{k+1}, \quad I_2 = \frac{x_{i+1}^{k+2} - x_i^{k+2}}{k+2}, \\ I_3 &= \frac{x_{i+1}^{k+3} - x_i^{k+3}}{k+3}, \quad I_4 = \frac{x_{i+1}^{k+4} - x_i^{k+4}}{k+4}, \end{aligned} \tag{35}$$

one obtains

$$\begin{aligned}\int_{x_1}^{x_{n+1}} & x^k s^{(3)}(x)\,\mathrm{d}x \\ &= \sum_{i=1}^{n} [I_1 s_{i0} + (I_2 - x_i I_1) s_{i1} + (I_3 - 2x_i I_2 + x_i^2 I_1) s_{i2} \\ &\quad + (I_4 - 3x_i I_3 + 3x_i^2 I_2 - x_i^3 I_1) s_{i3}]. \end{aligned} \tag{36}$$

This expression has to be the same as the kth moment μ_k of f, $k = 0, 1, \ldots$.

Now, a $4n \times 4n$ linear system of equations has been obtained and can be solved. The simplifications corresponding to linear and quadratic splines are straightforward.

Remark 4.1 (*Other boundary conditions*). In the case of boundary conditions other than (27) or (29), one can change the splines in the first or in the last interval. For instance, if only $s_1(x_1) = 0$ is known but nothing about the first and second derivative on the left boundary, one can use a first-order spline in the first interval. With the ansatz

$$s_1(x) = s_{10} + s_{11}(x - x_1) + 0(x - x_1)^2 + 0(x - x_1)^3, \tag{37}$$

the conditions (28) have to be replaced by

$$s_1(x_1) = s_{10} = 0, \quad s_{12} = 0, \quad s_{13} = 0. \tag{38}$$

4.2. Details of the algorithm, treatment of difficulties

The mathematical and numerical problems in the reconstruction of a distribution by splines are the following:

1. It is crucial to compute the reconstruction in an interval $[x_1, x_{n+1}] \supset \mathrm{supp}(f(x))$ such that $\mathrm{meas}[x_1, x_{n+1}] \backslash \mathrm{supp}(f(x))$ is small. This means, one has to find an interval for the reconstruction which is as small as possible.
2. Since the reconstruction should be an approximation of a probability density distribution, its values should be non-negative.
3. The linear system of equations which arises in this approach is ill-conditioned. The condition number grows (rather rapidly) towards infinity as the number of used moments increases.

To treat these problems, the reconstruction will be computed iteratively starting from an initial reconstruction $f^{(0)}(x)$ in an initial interval $[x_1^{(0)}, x_{n+1}^{(0)}]$.

Let $f^{(k)}(x)$ be a computed reconstruction in $[x_1^{(k)}, x_{n+1}^{(k)}]$. Each subinterval is divided into 10 equidistant smaller intervals with the nodes x_{ij}, $i = 1, \ldots, n$, $j = 1, \ldots, 10$, $x_{i1} = x_i$ and $x_{n+1,1} = x_{n+1}$. The maximum of the current reconstruction is denoted by

$$f_{\max}^{(k)} := \max \left\{ \max_{i=1,\ldots,n;\ j=1,\ldots,10} \{|f^{(k)}(x_{ij})|\}, |f^{(k)}(x_{n+1})| \right\}. \tag{39}$$

Treatment of problem 1: After having computed a reconstruction $f^{(k)}(x)$ in an interval $[x_1^{(k)}, x_{n+1}^{(k)}]$, it will be checked if the values of $f^{(k)}(x)$ are small in the subintervals $[x_1^{(k)}, x_2^{(k)}]$ and $[x_n^{(k)}, x_{n+1}^{(k)}]$, respectively. To do this, these subintervals are divided into 10 smaller subintervals and the values of $f^{(k)}(x)$ are computed in the nodes of these smaller subintervals (11 values in $[x_1^{(k)}, x_2^{(k)}]$ and $[x_n^{(k)}, x_{n+1}^{(k)}]$, respectively). Then it is checked if the values of $f^{(k)}$ in these intervals are sufficiently small compared to the maximal value of $f^{(k)}$. Considering for brevity only the right boundary, it is checked if

$$\left(\sum_{j=1}^{10} [(f^{(k)}(x_{nj}))^2 + (f^{(k)}(x_{n+1}^{(k)}))^2] \right)^{1/2} \leqslant \mathrm{tol}_{\mathrm{red}} f_{\max}^{(k)}. \tag{40}$$

If this criterion is fulfilled, we set $x_{n+1}^{(k+1)} := (x_n^{(k)} + x_{n+1}^{(k)})/2$, else $x_{n+1}^{(k+1)} := x_{n+1}^{(k)}$. In the numerical tests presented in this paper, the tolerance was set to be $\mathrm{tol}_{\mathrm{red}} = 0.01$. After having defined the interval $[x_1^{(k+1)}, x_{n+1}^{(k+1)}]$, the nodes are distributed again equidistantly within the new interval.

Treatment of problem 2: This problem is treated in close connection with the treatment of problem 3. For each reconstruction step leading to $f^{(k)}(x)$, it will be checked if all values at the nodes x_i $(i = 0, \ldots, n+1)$, and at the midpoints of the subintervals $x_{i6} = (x_i + x_{i+1})/2$ $(i = 0, \ldots, n)$, are (almost) non-negative:

$$\begin{aligned} f_{\min,\max} &:= \min_{j=1,\ldots,k} f_{\max}^{(j)}, \quad \frac{f^{(k)}(x_i)}{f_{\min,\max}} \geqslant \mathrm{tol}_{\mathrm{neg}} \\ &\text{and} \quad \frac{f^{(k)}(x_{i6})}{f_{\min,\max}} \geqslant \mathrm{tol}_{\mathrm{neg}}, \end{aligned} \tag{41}$$

with $\mathrm{tol}_{\mathrm{neg}} \leqslant 0$. Note that the reconstruction might be more negative between the nodes and the midpoints of the subintervals.

In our numerical studies, it could be observed that the result of the reconstruction process is sometimes sensitive to the choice of $\mathrm{tol}_{\mathrm{neg}}$. Quite often, a very small negative value for $\mathrm{tol}_{\mathrm{neg}}$ leads to a considerably better result than setting $\mathrm{tol}_{\mathrm{neg}} = 0$.

If (41) is not fulfilled and if the nodes will not be redistributed, a regularization is applied, as described below.

Treatment of problem 3: This problem is treated by regularizing the linear system of equations by neglecting small singular values. Therefore, the pseudoinverse routine of

MATLAB is used for computing a least-squares solution of the linear system $Ax = b$. The pseudoinverse routine of MATLAB treats all singular values of A which are smaller than a prescribed tolerance tol_{sing} as zero values. Neglecting small singular values removes oscillations from the solution. The strategy which was implemented for the numerical tests presented below is as follows:

- The initial tolerance is set to be $\text{tol}_{\text{sing}} = 1e-36$. Practically, no positive singular value is set to zero in this case.
- After each redistribution of the nodes, tol_{sing} is reset to its initial value.
- If criterion (41) is not fulfilled, the singular value σ of A with $\sigma > \text{tol}_{\text{sing}}$ which is closest to tol_{sing} is sought. Then, this singular value will be neglected in the next computation of the pseudoinverse of A by setting

$$\text{tol}_{\text{sing}} = \frac{\sigma + \tilde{\sigma}}{2}, \tag{42}$$

  where $\tilde{\sigma}$ is the smallest singular value of A which is larger than σ.
- The differentiability of splines with $l > 1$ is necessary to have sufficient equations for defining the spline. However, for the PSD, the continuity is the only important condition. To weaken the differentiability conditions, the related equations are multiplied with a constant ω^i, where i is the order of the differentiability condition. The effect of this scaling is that the equations describing higher differentiability are neglected first in the truncation of the singular values.

Another method which helped considerably to decrease the numerical instabilities is an appropriate scaling of the domain and of the moments within the computations. This avoids performing the computations with numbers showing a very large difference in the order of magnitude, for example from 1 to $1e-33$ (see Section 2). Let the data be for example non-zero only within $[a, b]$ with

$$\int_a^b x^l f(x)\,\mathrm{d}x = \mu_l, \quad l = 0, 1, \ldots . \tag{43}$$

By introducing $y = \alpha x$, the integral is transformed to

$$\int_{\alpha a}^{\alpha b} y^l f\left(\frac{y}{\alpha}\right)\mathrm{d}y = \alpha^{l+1}\mu_l, \quad l = 0, 1, \ldots . \tag{44}$$

Instead of reconstructing the probability density distribution $f(x)$ for $x \in [a, b]$ from the moments μ_l, it is preferable to reconstruct $f(y/\alpha)$ for $y \in [\alpha a, \alpha b]$ from the moments $\alpha^{l+1}\mu_l$, where α is chosen appropriately, see the numerical studies.

Furthermore, the moments are always normalized within the computations by using

$$\int_{\alpha a}^{\alpha b} y^l \frac{f(y/\alpha)}{\alpha\mu_0}\,\mathrm{d}y = \alpha^l \frac{\mu_l}{\mu_0}, \quad l = 0, 1, \ldots . \tag{45}$$

In this way, the 0th moment of the function $f(y/\alpha)/(\alpha\mu_0)$ is always normalized to 1.

The iteration for reconstructing the probability density function will finally be stopped automatically if the criterion (41) is fulfilled and no redistribution of the nodes is recommended.

4.3. Numerical studies

Considering the reconstruction of a probability density distribution using splines, some parameters can be freely chosen by the user, for instance the number of moments used for reconstruction, the value of tol_{neg} and the initial interval $[x_1^{(0)}, x_{n+1}^{(0)}]$. Under normal conditions, it will not be difficult to determine appropriate values, but an improper choice of these parameters might of course influence the convergence process and/or the results. Due to the limited length of this paper it is not possible to present systematic studies. Nevertheless, all the values employed for the test-cases are listed below.

The iterative algorithm has already been briefly demonstrated in John et al. (2005), Fig. 5. The number of iterations needed to obtain the results presented below depends on the difficulty of the considered example and on the degree of the spline. Often, only a few iterations are necessary. The most difficult case considered here required less than 50 iterations. As a general rule, the reconstruction needs more iterations when increasing the degree of the spline. For all cases, the spline-based reconstruction took less than 30 s on a standard PC, which is a negligible short time compared to the time needed to obtain the moments.

Using the transformation described above, the initial domain within the computations was always the interval $[0, 1]$. The scaling parameter of the differentiability conditions was fixed to $\omega = 10^{-4}$.

Example 2.1: First, we present results for the minimal number of moments which are necessary to reconstruct the global shape of the distribution (Fig. 7). For this example these have been found to be $(\mu_0, \ldots, \mu_6)$ for the linear spline, $(\mu_0, \ldots, \mu_5)$ for the quadratic spline and (μ_0, μ_1, μ_2) for the cubic spline.

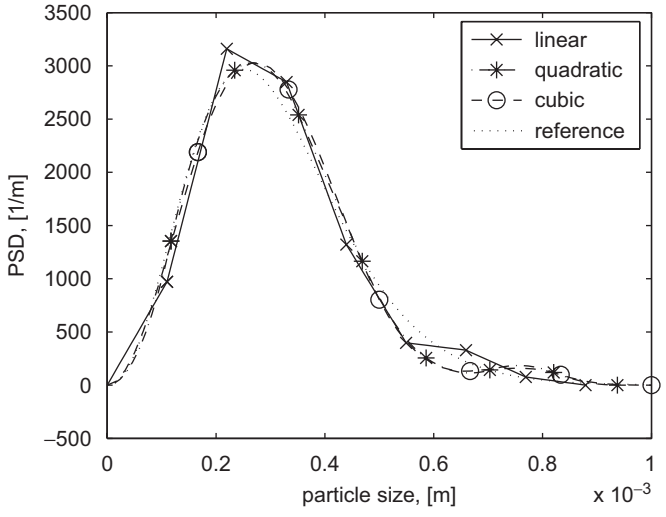

Fig. 7. Example 2.1, reconstruction of the distribution with seven moments for the linear spline, six moments for the quadratic spline and three moments for the cubic spline.

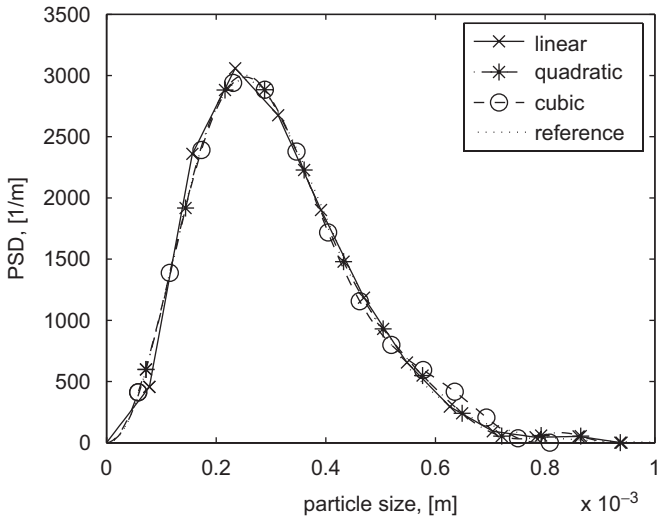

Fig. 8. Example 2.1, reconstruction of the distribution with 11 moments.

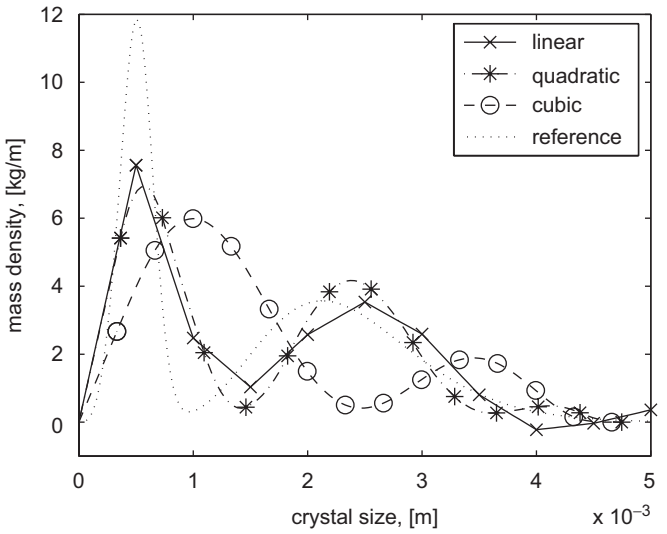

Fig. 9. Example 2.2, reconstruction of the distribution with 11 moments.

The parameters of the computations are $\text{tol}_{\text{neg}}=0$, $[x_1^{(0)}, x_{n+1}^{(0)}]=[0, 1e-3]$ and the boundary conditions (27) and (29).

The results obtained when using always the first 11 moments are presented in Fig. 8. The parameters for these computations are $[x_1^{(0)}, x_{n+1}^{(0)}] = [0, 1.5e-3]$ and $\text{tol}_{\text{neg}} = 0$. One can see that the algorithm finds automatically the region of interest and reduces the interval for the reconstruction appropriately. One obtains almost perfect reconstructions with all splines. Only the cubic spline shows a small difference compared to the reference distribution at $x \approx 0.65$ mm.

The reason for this behavior might be the smaller reliability (higher round-up error) of the higher moments. Since the reference solution is given only as a set of discrete points, a spline interpolation is used to compute the moments listed for Example 2.1 by numerical quadrature. Thus, the available values are not perfectly accurate since one always has to interpolate between the discrete points of the reference distribution.

Example 2.2: The results for this example are presented in Fig. 9. They have been obtained using 11 moments $(\mu_0, \ldots, \mu_{10})$, $[x_1^{(0)}, x_{n+1}^{(0)}] = [0, 1e-2]$, $\text{tol}_{\text{neg}} = -0.05$ for the linear spline, $\text{tol}_{\text{neg}} = -0.001$ for the other splines and the boundary conditions (38) and (29).

All splines identify the correct number of peaks (two). Furthermore, the linear and the quadratic spline reconstruction detect the positions of these peaks reasonably well. However, the height of the left peak of the reconstruction is too small. Since this peak is quite narrow, there are not enough grid points inside the peak to resolve its height correctly. The reconstruction with the cubic spline is even worse. The reason is the boundary condition on the left-hand side. Using the smooth transition condition (27), there are not enough grid points in the interval $[0, 1e-3]$ to resolve the large curvatures of the narrow peak. The boundary condition (38), which uses a linear spline in the first interval, leads to the condition of a vanishing second derivative at the grid point x_2. The cubic spline in $[x_2, x_3]$ has to have also a vanishing second derivative at x_2. To follow the peak, however, requires a non-zero curvature in x_2, leading to an incompatible condition. A remedy consists in using a quadratic spline in $[x_2, x_3]$, which does not have to obey any condition on the second derivative in x_2 imposed by the linear spline in $[x_0, x_1]$, before later on switching to the cubic spline.

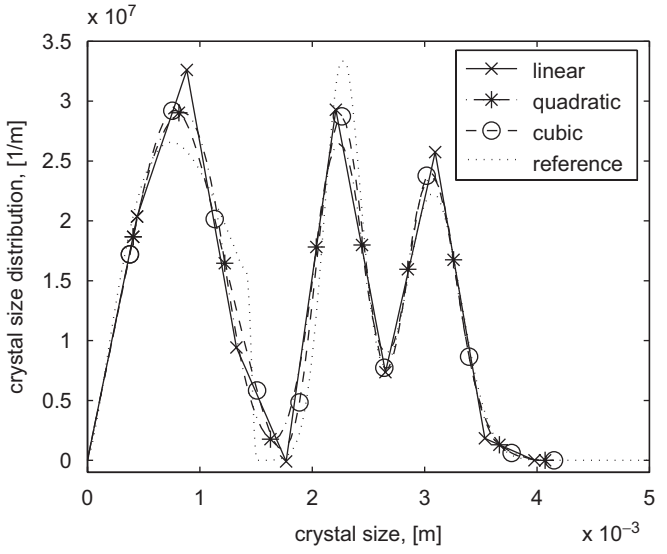

Fig. 10. Example 2.3, reconstruction of the distribution with eight moments.

The concentration of grid points in regions of interest and the use of different order splines in different intervals is the subject of forthcoming studies, as explained at the end of this section.

Example 2.3: The results for the distribution with three peaks are presented in Fig. 10. In these computations, eight moments have been employed $(\mu_0, \ldots, \mu_7)$ with $[x_1^{(0)}, x_{n+1}^{(0)}] = [0, 5e-3]$, $\text{tol}_{\text{neg}} = -0.01$ and the boundary conditions (38) and (29). The results are quite close to the reference curve. Despite the fact that no a priori information on the shape of the reference distribution has been used, all spline reconstructions directly

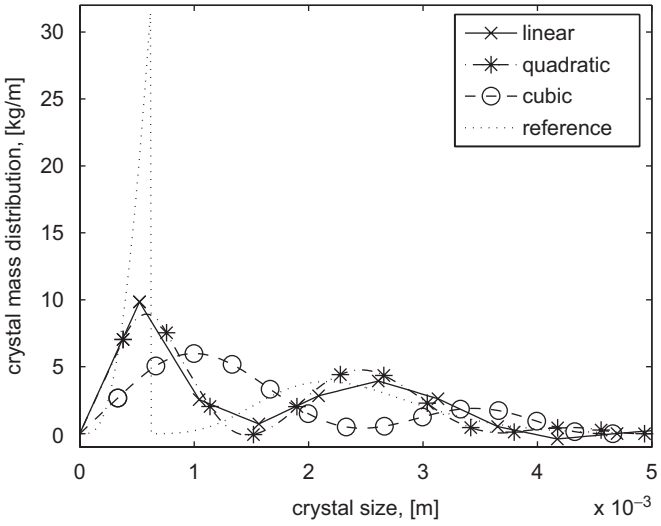

Fig. 11. Example 2.4, reconstruction of the distribution with 11 moments.

recover the three peaks. On the other hand, the splines are not able to perfectly reconstruct the steep drop down of the crystal size distribution around $x = 1.6$ mm. They are smoother than the reference distribution and resemble the results presented for the backward-difference method in Fig. 5.

Example 2.4: This is the most difficult example for the reconstruction, see Fig. 11 for a support of this statement, since the reference distribution shows a very sharp front at $x \approx 0.6$ mm, with two completely different peaks: the first one is very high and narrow, the second one quite small but broad.

The linear and quadratic spline reconstruction show two peaks which are roughly at the correct positions. But the first peak of the reconstruction is much too small. The reconstruction with the cubic spline shows also the correct number (two) of peaks, however, too far on the right-hand side. The reasons for the insufficient height of the first peak in the linear and quadratic spline reconstruction as well as the results of the cubic spline reconstruction are the same as given for Example 2.2. The non-smooth behavior of the distribution is not detected.

The parameters for the results presented in Fig. 11 are the use of all 11 moments $(\mu_0, \ldots, \mu_{10})$, $[x_1^{(0)}, x_{n+1}^{(0)}] = [0, 1e-2]$, $\text{tol}_{\text{neg}} = -0.05$ for the linear spline, $\text{tol}_{\text{neg}} = -0.01$ for the quadratic and cubic spline and the boundary conditions (38) and (29).

4.4. Possible improvements

The reconstruction of a smooth distribution with splines works quite well and efficiently. Besides the examples given above, good results have been also obtained, for example, for the reconstruction of the sum of two Gaussian curves. Reconstructing a non-smooth distribution or a distribution with narrow and steep peaks is much more challenging.

It is thus appropriate to emphasize again the two main reasons for the results shown in Examples 2.2 and 2.4 since they offer the directions in which the algorithm can be extended and improved. First, the quadratic and the cubic spline are smooth by construction. In our algorithm, the smoothness conditions are already partly relaxed by the scaling factor ω, see the treatment of problem 3. However, one cannot reasonably expect a good reconstruction of a non-smooth distribution by a smooth ansatz. The second reason is the equi-distribution of the nodes. For reconstructing correctly the narrow peak at the left-hand side of the distributions, more nodes should be concentrated in this region.

Topics for further studies thus include:

- The use of non-equidistant grids. The nodes should be concentrated in regions of interest, e.g., with large curvature, by using an a posteriori error estimator.
- Using splines with a different order of the polynomials in the subintervals, in order to handle situations where the probability density distribution is locally not smooth.
- Studying different approaches for the regularization, which might be more efficient than the truncation of the singular value decomposition.

The first two topics are in our opinion the most important ones. But it is already possible to use the available algorithm with a good accuracy for a large variety of practical problems, as demonstrated for several examples considered in this section.

5. Summary

The reconstruction of a probability density distribution using a finite number of its moments is an ill-posed inverse problem. Several reconstruction approaches have been introduced, discussing their advantages, drawbacks and perspectives. Three different approaches have been then evaluated on probability density distributions arising typically in chemical engineering applications.

The reconstruction by parameter fitting using a priori prescribed shape functions is currently the most popular approach because of its simplicity. This will probably not change in the near future. However, this approach can only be used if the shape of the distribution is known in advance, if the distribution has a simple shape or if additional information on the distribution are available.

The efficiency of the discrete method has been demonstrated on two examples. The main restriction of the discrete method so far is that it is only applicable to simple population models, where the distribution is influenced only by growth and birth processes. Further investigations are needed to investigate the possible extension of this approach to problems including phenomena like breakage, agglomeration, attrition, etc.

The spline reconstruction presented in the last section is a general and flexible approach, which requires no a priori knowledge about the distribution to reconstruct. A first working version of this approach has been presented in detail, using equidistant grids and equal-order splines in each interior interval. This approach has been proved to be fully sufficient to reconstruct smooth distributions accurately and efficiently. Possible improvements have been identified and are presently being implemented in order to better deal for example with narrow peaks near the boundary or local non-smooth behavior.

Acknowledgment

A. Öncül and D. Thévenin would like to thank Pro3, the German Process Engineering Expertise Network, for its financial support during part of this work.

References

Bałdyga, J., Bourne, R., 1999. Turbulent Mixing and Chemical Reactions. Wiley, New York.

Bałdyga, J., Orciuch, W., 2001. Barium sulphate precipitation in a pipe: an experimental study and CFD modelling. Chemical Engineering Science 56, 2435–2444.

Bandyopadhyay, K., Bhattacharya, A.K., Biswas, P., Drabold, D.A., 2005. Maximum entropy and the problem of moments: a stable algorithm. Physical Review E 71, 057701/1–057701/4.

Berkov, D.V., Gœrnert, P., Buske, N., Gansau, C., Mueller, J., Giersig, M., Neumann, W., Su, D., 2000. New method for the determination of the particle magnetic moment distribution in a ferrofluid. Journal of Physics D 33, 331–337.

Bertero, M., De Mol, C., Pike, R., 1985. Linear inverse problems with discrete data I. Inverse Problems 1, 301–330.

Chebyshev, P., 1961. Sur les valeurs limites des intégrales. Oeuvres, New York.

Chen, J., Zheng, C., Chen, G., 1996. Interaction of macro- and micromixing on particle size distribution in reactive precipitation. Chemical Engineering Science 51, 1957–1966.

Diemer, R.B., Ehrman, S.H., 2005. Pipeline agglomerator design as a model test case. Powder Technology 156, 129–145.

Diemer, R.B., Olson, J.H., 2002. A moment methodology for coagulation and breakage problems: part 2—moment models and distribution reconstruction. Chemical Engineering Science 57, 2211–2228.

Elsner, M.P., Fernández Menéndez, D., Alonso Muslera, E., Seidel-Morgenstern, A., 2005. Experimental study and simplified mathematical description of preferential crystallization. Chirality 17 (S), 183–195.

Fox, R.O., 1998. On the relationship between lagrangian micromixing models and computational fluid dynamics. Chemical Engineering Proceedings 37, 521–535.

Frontini, M., Rodriguez, G., Seatzu, S., 1988. An algorithm for computing minimum norm solutions of finite moment problems. In: Mason, J.C., Cox, M.G. (Eds.), Algorithms for Approximation. Chapman and Hall, London, pp. 361–369.

Giaya, A., Thompson, R.W., 2004. Recovering the crystal size distribution from the moment equations. A.I.Ch.E. Journal 50 (4), 879–882.

Gzyl, H., 2000. Maxentropic reconstruction of some probability distributions. Studies in Applied Mathematics 105 (3), 235–243.

Heinz, S., 2003. Statistical Mechanics of Turbulent Flows. Springer, Berlin.

Hulburt, H.M., Katz, S., 1964. Some problems in particle technology: a statistical mechanical formulation. Chemical Engineering Science 19, 555–574.

Inglese, G., 1988. Approximate solutions for a finite moment problem. Calcolo 25, 233–248.

Inglese, G., 1994. A note about the discretization of finite moment problems. Inverse Problems 10, 401–414.

Inglese, G., 1995. Christoffel functions and finite moment problems. Inverse Problems 11, 949–960.

John, V., Angelov, I., Öncül, A.A., Sundmacher, K., Thévenin, D., 2005. Towards the optimal reconstruction of a distribution from its moments. In: A.I.Ch.E. Annual Meeting, Paper 287, Cincinnati, USA, ISBN 3-86010-797-6.

Marchisio, D.L., Fox, R.O., 2005. Solution of population balance equations using the direct quadrature method of moments. Journal of Aerosol Science 36, 43–73.

Marchisio, D.L., Fox, R.O., Barresi, A.A., Garbero, M., Baldi, G., 2001. On the simulation of turbulent precipitation in a tubular reactor via computational fluid dynamics. Chemical Engineering Research and Design 79, 998–1004.

Marchisio, D.L., Barresi, A.A., Garbero, M., 2002. Nucleation growth and agglomeration in barium sulfate turbulent precipitation. A.I.Ch.E. Journal 48, 2039–2050.

McGraw, R., 1997. Description of aerosol dynamics by the quadrature method of moments. Aerosol Science and Technology 27, 255–265.

McGraw, R., Nemesure, S., Schwatz, S.E., 1998. Properties and evolution of aerosols with size distributions having identical moments. Journal of Aerosol Science 29 (7), 761–772.

Mersmann, A., 2001. Crystallization Technology Handbook. second ed.. Marcel Dekker Inc., New York.

Myers, K.J., Hanson, K.M., 1990. Comparison of the algebraic reconstruction technique with the maximum entropy reconstruction technique for a variety of detection tasks. Proceedings of the SPIE 1231, 176–187.

Öncül, A.A., Elsner, M.P., Thévenin, D., Seidel-Morgenstern, A., 2005a. Numerical analysis of the preferential crystallization of enantiomers in complex flows. In: 12th International Workshop on Industrial Crystallization BIWIC2005, Halle, Germany, pp. 165–172, ISBN 3-86010-797-6.

Öncül, A.A., Thévenin, D., Elsner, M.P., Seidel-Morgenstern, A., 2005b. Numerical analysis of the preferential crystallization of enantiomers. In: Sommerfeld, M. (Ed.), 11th Workshop on Two-Phase Flow Predictions, Halle, Germany, pp. 5.10/15.10/15, ISBN 3-86010-767-4.

Öncül, A.A., Sundmacher, K., Seidel-Morgenstern, A., Thévenin, D., 2006. Numerical and analytical investigation of barium sulphate crystallization. Chemical Engineering Science 61, 652–664.

Qamar, S., Elsner, M.P., Angelov, I.A., Warnecke, G., Seidel-Morgenstern, A., 2006. A comparative study of high resolution schemes for solving population balances in crystallization. Computers and Chemical Engineering 30 (6–7), 1119–1131.

Randolph, A.D., Larson, M.A., 1988. Theory of Particulate Processes. Academic Press Inc., New York.

Ramkrishna, D., 2000. Population Balances: Theory and Applications to Particulate Systems in Engineering. second ed., Academic Press, A Harcourt Science and Technology Company.

Sanyal, J., Marchisio, D.L., Fox, R.O., Dhanasekharan, K., 2005. On the comparison between population balance models for CFD simulation of bubble columns. Industrial Engineering Chemistry Research 44, 5063–5072.

Shohat, J.A., Tamarkin, J.D., 1943. The problem of moments. AMS Mathematical Survey, vol. 1. AMS, Providence, RI.

Sluzek, A., 2005. On moment-based local operators for detecting image patterns. Image and Vision Computing 23, 287–298.

Tagliani, A., 1999. Hausdorff moment problem and maximum entropy: a unified approach. Applied Mathematics and Computation 105, 291–305.

Tagliani, A., 2001. Numerical aspects of finite Hausdorff moment problem by maximum entropy approach. Applied Mathematics and Computation 118, 133–149.

Talenti, G., 1987. Recovering a function from a finite number of moments. Inverse Problems 3, 501–517.

von Smoluchowski, M., 1917. Versuch einer mathematischen Theorie der Koagulationskinetik kolloider Lösungen. Zeitschrift fur Physikalische Chemie 92, 129–168.